Optimization of hybrid coagulation-ultrafiltration process for potable water treatment using response surface methodology

S. G. Arhin, N. Banadda, A. J. Komakech, W. Pronk and S. J. Marks

ABSTRACT

In order to optimize the operating conditions for a combined polyaluminum chloride (PACl) coagulation/flocculation and ultrafiltration process for treating potable water, the main, second order and interaction effects of PACl dose and flocculation retention time (FRT) on permeate turbidity, UV_{254} and membrane permeability were investigated using a 100 kDa hollow fiber membrane operated in the dead-end mode. A multilevel factorial design was used to determine the relevant ranges of the two factors for optimization. A 2^2 central composite design (CCD) was then used to develop mathematical correlation models for the optimum operating conditions. The main effect of PACl dose was the most significant factor on all the responses. For permeability, both the main effect of FRT and FRT–PACl dose interactions were found to be insignificant. The optimum PACl dose and FRT for the feed water were 20 mg/L and 14 min, respectively. Corresponding permeate turbidity, UV_{254} and permeability were 0.15 ± 0.01 NTU, 0.003 ± 0.001 cm^{-1} and 62.0 ± 9.52 Lm^{-2} h^{-1} bar^{-1}, respectively. Experimental validation runs confirmed the reliability of the predicted optimal conditions thus implying that CCD models can be used to predict/optimize the quality and quantity of permeate from hybrid coagulation–ultrafiltration systems for potable water treatment.

Key words | central composite design, coagulation, optimization, polyaluminum chloride, ultrafiltration

S. G. Arhin (corresponding author)
N. Banadda
A. J. Komakech
Department of Agricultural and Biosystems
     Engineering,
Makerere University,
P.O. Box 7062,
Kampala,
Uganda
E-mail: *arhinsamuel32@gmail.com*

S. G. Arhin
W. Pronk
S. J. Marks
Eawag: Swiss Federal Institute of Aquatic Science
     and Technology,
Überlandstrasse 133,
Dübendorf 8600,
Switzerland

INTRODUCTION

Ultrafiltration (UF) is widely applied as an effective technique for removing a diverse array of waterborne pathogens such as protozoa, bacteria and viruses from drinking water (Hill *et al.* 2007; Mull & Hill 2012). At the appropriate molecular weight cut-off (MWCO), UF membranes can produce bacteria-free drinking water, remove greater than 6 log of viruses, turbidity, a portion of natural organic matter (NOM) and disinfection byproduct precursors from the feed water (Liang *et al.* 2008; Mimoso *et al.*

2015). Compared with conventional sand filtration, UF has several advantages which include a higher treatment efficiency, smaller footprint, fewer chemicals demand, less sludge production and easy automation. Furthermore, recent advances in membrane technology have made UF a cost-effective alternative to other filtration techniques (Jeong *et al.* 2012; Mull & Hill 2012). It is therefore seen by communities as a safer treatment alternative (Guo *et al.* 2009).

Despite these advantages, membrane fouling still remains an important limitation for this technology (Arhin *et al.* 2016). Membrane fouling occurs when organic and inorganic matter retained by the membrane accumulate on

the membrane surface or within the membrane pores generating an increasing hydraulic resistance. Fouling reduces hydraulic permeability, increases transmembrane pressure and cleaning frequencies, which eventually lead to higher operating costs. Moreover, frequent membrane cleaning operations may lead to membrane deterioration causing reduction in the permeate quality and shorter membrane life span (Chon *et al.* 2012; Munla *et al.* 2012; Xu *et al.* 2014). In order to minimize fouling, pretreatment of feed water using techniques such as coagulation, adsorption, oxidation, bio-filtration, magnetic ion exchange resins and integrated pretreatment is practiced in full-scale and pilot-scale UF plants (Gao *et al.* 2011). Among the various pretreatment techniques, coagulation is the most dominantly used due to its low cost, ease of operation and ability to significantly improve UF performance (Arhin *et al.* 2016). It is presumed that during coagulation, colloids are destabilized and clusters form larger flocs which are easily retained by UF membranes (Xiangli *et al.* 2008). Besides fouling minimization, the use of coagulation pretreatment has an additional beneficial effect since it can improve the removal efficiency of harmful contaminants such as viruses (Fiksdal & Leiknes 2006; Konieczny *et al.* 2006).

Although coagulation pretreatment is rapidly gaining attention, research evaluating its effect on membrane fouling has been inconsistent. Whereas several studies have reported improved membrane performance with coagulation pretreatment (Dong *et al.* 2007; Kimura *et al.* 2014; Lai *et al.* 2015), others observed decreased or no improvement in membrane performance (Maartens *et al.* 1999; Howe & Clark 2006). The inconsistencies in coagulation pretreatment have been attributed to several factors such as the specific characteristics of the feed water and properties of NOM, type of membrane material and the module configuration, flow configuration (dead-end or cross-flow), running mode (constant pressure or constant flux), type of coagulant, dose used, whether coagulation was performed with or without flocculation, the retention time used for flocculation and whether there was sedimentation prior to filtration (Arhin *et al.* 2016). Among these factors, the coagulant dose and the flocculation retention time (FRT) are two factors that have a significant impact on operational costs (Li *et al.* 2011). These two factors can influence floc formation and the size distribution of flocs, which affect both

hydraulic permeability and solute rejection. Moreover, the floc size required in hybrid coagulation-UF systems is not necessarily the same as the floc size required for conventional coagulation because UF membranes are able to retain even small flocs. It is therefore imperative that the coagulant dose and FRT are optimized with regards to membrane performance.

In recent years, response surface methodology (RSM) has become very popular for simultaneous optimization and modelling of chemical processes (Bas & Boyaci 2007; Bezerra *et al.* 2008). RSM is a collection of statistical and mathematical techniques used to predict and optimize a response or set of responses of interest by adjusting several variables. The main advantage of RSM is that it includes interaction effects among the variables and, thus, depicts the complete effects of the variables on the response unlike the classical one-variable-at-a-time optimization approach where the desired response is obtained by keeping all other variables at a constant level (Prasad *et al.* 2011). In addition to that, it reduces the number of experimental trials needed to evaluate multiple variables and their interactions, thereby saving time and expenses (Sharma *et al.* 2009). Yet, most studies optimizing the operating conditions for hybrid coagulation–membrane filtration process have not considered the possibility of using RSM.

Previous studies such as Zularisam *et al.* (2009) delivered very relevant insights about optimization of alum towards NOM removal and membrane permeability amelioration. Nowadays, there is a growing interest in the use of pre-hydrolyzed coagulants such as polyaluminum chloride (PACl) over alum for coagulation pretreatment. PACl contains highly charged tridecamer cationic species (Al_{13}) which are strongly absorbed on negative colloids (Duan & Gregory 2003). There are several benefits of PACl over alum such as the ability to form more robust flocs, lower aluminum residuals in treated water, reduced sludge volumes and improved performance under low temperature regimes (Arhin *et al.* 2016). Aside from that, in addition to NOM removal, it is also important to consider the influence of coagulation on the nexus between turbidity and reversible fouling as turbidity spikes affect plant operational and maintenance regimes such as backflush flux and frequency, chemical cleaning protocol and transmembrane pressure which in tend influence fouling rates and productivity

(Amy 2008; Hatt *et al.* 2011). Moreover, some studies have demonstrated fouling suppression at coagulant doses not significantly influencing NOM removal, thus suggesting flux amelioration is not contingent upon NOM removal (Choi & Dempsey 2004; Konieczny *et al.* 2009).

In this study, the optimum operating conditions for a hybrid PACl coagulation-UF system for potable water treatment were determined using RSM. The focus of this study was to establish the optimum PACl dose and FRT for enhancing both organic and inorganic foulants removal. To that end, the independent variables considered were PACl dose and FRT, and the process output was assessed in terms of UV_{254} removal: used as a surrogate for NOM, especially for humic acids (Cho *et al.* 2006), turbidity removal: used as an indicator for particulate matter (Kim *et al.* 2007) and membrane permeability. Preliminary batch experiments (jar tests) were performed to test the relevance of the variables on the feed water and to determine their ranges for optimization. Thereafter by means of RSM, the optimum PACl dose and FRT were determined. This study provides insights into quantitative identification and simultaneous optimization of significant variables for hybrid coagulation-UF systems.

MATERIALS AND METHODS

Raw water sampling and samples characterization

Surface water samples from Lake Victoria were collected at the raw water inlet to Ggaba II Water Treatment Works, Kampala, Uganda from November 2015 to April 2016. Daily sampling was done between 8:00 and 9:00 am. Analytical tests were conducted to characterize the raw water based on temperature, pH, electrical conductivity, turbidity, color, and UV_{254}. Temperature was determined with an Extech MO295 IR thermometer (Extech® instruments, USA). pH and conductivity were determined using Hach Sension + MM374 multi parameter meter (Hach, USA). A turbidimeter (Hach 2100Q, USA) was used for turbidity measurements and a UV spectrophotometer (Hach DR1900, USA) was used for color determination at 455 nm. Another UV spectrophotometer (photoLab 6600 UV-VIS; WTW, Germany) was used for UV_{254}. Following

standard procedure, samples for UV_{254} analysis were filtered with 0.45 μm sterile filter membranes (MCNE-447-100; Labbox, France) prior to analysis (USEPA 2003). Samples which could not be analyzed on the day of sampling were kept at a temperature of +4 °C (Gamage & Chellam 2011). No sample was kept for more than 3 days without performing analysis. Table 1 summarizes the characteristics of the feed water used for the study. Each parameter was determined at least in triplicate.

Preliminary batch experiments

Preliminary experiments were done to verify the statistical relevance of the two independent variable (PACl dose and FRT) and to determine their experimental ranges for optimization (Choi & Dempsey 2004; Cho *et al.* 2006; Bas & Boyaci 2007). A multilevel factorial design consisting of two factors, 24 base runs and three replicates was used to determine the statistical significance of PACl dose and FRT on the quality of water from Lake Victoria. The supernatant turbidity, UV_{254} and color were used to denote the quality characteristics. A six paddle jar test apparatus (Stuart Scientific Flocculator; SW1, UK) was used to study the change in particle size during coagulation. Tests were executed following standard protocol (ASTM 2013). Commercial PACl in liquid form (Zetafloc 553 l) was purchased from Abby Laboratories, South Africa. The stock solution was prepared by dosing one mL of the coagulant in 100 mL of distilled water. Coagulation/flocculation was done in 1,000 mL Griffin beakers. The multiple stirrer was started at a speed of 120 rpm and coagulant doses corresponding to 10, 12, 14, 16, 18, and 20 mg/L were added without pH adjustment: previous studies have reported

Table 1 | Raw water quality of Lake Victoria

Parameter	Mean	Standard deviation
Temperature (°C)	24.7	1.4
pH	7.2	0.3
Conductivity (μS/cm)	120.6	2.1
Turbidity (NTU)	15.4	2.5
Color (PtCo)	177.0	17.0
UV_{254} (cm^{-1})	0.030	0.010

measureable fouling abatement within the pH range measured for the raw water used (Hatt *et al.* 2011). Rapid mixing was done for a minute after which the speed was reduced to 30 rpm. The experiment was performed under FRTs of 5, 10, 15, and 20 min. After slow mixing, the paddles were withdrawn and samples were settled for 15 min. Supernatant samples were then siphoned mid-way through the beakers for turbidity, color and UV_{254} analysis.

Membrane filtration

Commercially available hollow tube UF membranes were used. The membrane specifications are provided in Table 2. The experimental setup is schematically illustrated in Figure 1. As shown in Figure 1, the set-up consists of coagulation/flocculation process followed by UF without prior sedimentation (Bergamasco *et al.* 2011). The exper-

Table 2 | Membrane specification

Parameter	Membrane module
Membrane type	Hollow fiber
Supplier	Frontec Environmental Co., Ltd, China
Module configuration	Inside-out
MWCO	100 kDa
Module length	0.533 m
Membrane area	1.9 m^2

iment was conducted in the constant pressure mode so that any decline in permeate flux due to membrane fouling could be monitored effectively (Meng *et al.* 2006). A constant transmembrane pressure of 30 kPa was applied to extract permeate across the membrane in the dead-end mode. A speed variable peristaltic pump (AT300S + YT25 pump head; Dalian Tiancheng Machine Co. Ltd, China) was used to pump the coagulated water through the UF membrane at a constant pump speed. The pump served a dual function as feed and backwash pump.

The membrane permeate flow was determined by weighing permeate on a top-loading balance at timed intervals (Lai *et al.* 2015). The permeate flux was then obtained by dividing the permeate flow by the membrane surface area as shown in Equation (1):

$$J = \frac{Q}{A} \tag{1}$$

where Q is the permeate flow (L/h) and A is the membrane area (m^2). The membrane permeability – after 60 min of continuous filtration – was subsequently determined by dividing the flux by the transmembrane pressure as shown in Equation (2):

$$P = \frac{J}{TMP} \tag{2}$$

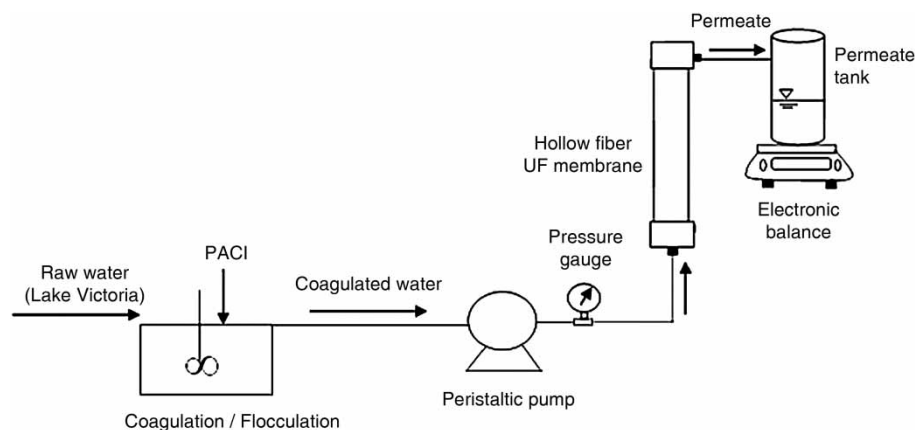where TMP is the transmembrane pressure (Pa).

Figure 1 | Schematic representation of the hybrid coagulation-UF process.

Experimental design for RSM

After the experimental ranges for the independent variables were obtained, RSM was used to determine the optimum factor settings for pre-coagulation. A 2^2 rotatable central composite design (CCD) consisting of factor combinations at two levels, four star points and five replicates at the center point was developed. The coagulant dose (coded as X_1) and FRT (coded as X_2) were set as the independent variables while the permeate turbidity (Coded as Y_1), UV_{254} absorbance (coded as Y_2) and the membrane permeability (coded as Y_3) were set as the response variables. Randomization of the experimental runs was done to limit the effects of unexpected variability in the response. Table 3 shows the range and levels of the two independent variables for the response surface design.

The experimental data from RSM was fitted into the polynomial model indicated in Equation (3):

$$Y = \beta_0 + \sum_{i=1}^{k} \beta_i X_i + \sum_{i=1}^{k} \beta_{ii} X_i^2 + \sum_{\substack{i=1 \\ i<j}}^{k-1} \sum_{j=i+1}^{k} \beta_{ij} X_i X_j \qquad (3)$$

where Y is the response variable; $X_1, X_2, ..., X_k$ are the independent variables affecting the response Y; β_0, β_i ($i = 1, 2, ..., k$), β_{ii} ($i = 1, 2, ..., k$) and β_{ij} ($i = 1, 2, ..., k; j = 1, 2, ..., k$) are the regression coefficients for intercept, linear, quadratic and interaction terms respectively; and k is the number of variables (Bas & Boyaci 2007; Silva *et al.* 2007).

After developing mathematical models for the response variables, the Derringer function (Murphy *et al.* 2005; Bezerra *et al.* 2008) was used to obtain a desirability function for each individual response (d_i; $0 \le d_i \le 1$), after which the overall desirability function (D), was computed as a weighted average of the individual desirability (d_i) according to Equation (4):

$$D = \sqrt[m]{d_1 d_2 \ldots d_m} \qquad (4)$$

where m is the number of responses.

The goal of the coagulation-UF process is to obtain a low turbidity and low UV_{254} (organics) in the permeate while maintaining a relatively high permeability across the UF membrane. Therefore, the desirability function for turbidity and UV_{254} were both the 'smaller-the-better' responses, which criterion is expressed in Equation (5) whereas the desirability function for permeability was the 'larger-the-better' response, which transformation is described in Equation (6):

$$d = \begin{cases} 1, & y < T \\ \left(\dfrac{U - y}{U - T}\right)^t, & T \le y \le U \\ 0, & y > U \end{cases} \qquad (5)$$

$$d = \begin{cases} 0, & y < 1 \\ \left(\dfrac{y - L}{T - L}\right)^t, & L \le y \le T \\ 1, & y > T \end{cases} \qquad (6)$$

where U is the upper acceptable value to the response, L is the lower acceptable value to the response, T is the target value, y is the response and t is the weight (Bezerra *et al.* 2008).

After the optimum conditions were obtained from the desirability function, four experimental replicates were performed at the optimal settings (Silva *et al.* 2007). The experimental and predicted values were subsequently compared to validate the response surface optimization.

Data analysis and statistical testing

Minitab 17.3.1 (Minitab®, USA) was used for statistical testing. All statistical tests were conducted at 95% confidence interval (CI). The statistical significance of mathematical correlation models was verified by Fisher's statistical test (F-test) for analysis of variance (ANOVA). Also, the coefficient of determination, R^2 was used as an indicator of the adequacy of the fitted polynomial model.

Table 3 | Independent variables and factor levels for response surface design

		Coded levels				
		−1.4	−1.0	0.0	+1.0	+1.4
Factors	Units	Natural levels				
Dose (X_1)	mg/L	7.0	10.0	15.0	20.0	22.0
FRT (X_2)	Min	3.3	5.0	10.0	15.0	17.0

RESULTS AND DISCUSSION

Preliminary jar test results

The statistical significance of PACl dose and FRT on turbidity, UV_{254} and color of the feed water was investigated and their relevant experimental ranges to consider for optimization were determined. As can be inferred from Table 4, both PACl dose and FRT were found to be significant factors affecting turbidity, UV_{254} and color. With the exception of UV_{254}, a *p*-value of 0.000 was computed for both PACl dose and FRT on all the responses indicating that these factors could highly influence the water quality. A similar observation was reported by Li *et al.* (2011) who claimed that among the factors affecting the hybrid coagulation – UF process, coagulant dose and retention time are two crucial factors that can impact on floc formation and size distribution as well as permeability of UF membranes. Thus, a remarkable improvement on the water quality coupled with improved membrane permeability could be attained if those two factors could be adjusted correctly.

Figure 2 shows the effect of varying PACl dose and FRT on turbidity, UV_{254} and color. As depicted in Figure 2(a), turbidity removal did not improve beyond 15 min. Even though, at 20 min FRT, a slight improvement was observed from 12 to 14 mg/L of the coagulant, a much turbid supernatant was attained afterwards. For UV_{254} and color, increasing the FRT to 20 min produced a much poorer supernatant quality. These results were consistent with the findings of Cho *et al.* (2006) who observed that at retention times larger than 20 min, there was no improvement in the removal of UV_{254}. Similarly, Li *et al.* (2011) noted that beyond 10 min retention time, no significant improvement in the removal of dissolved
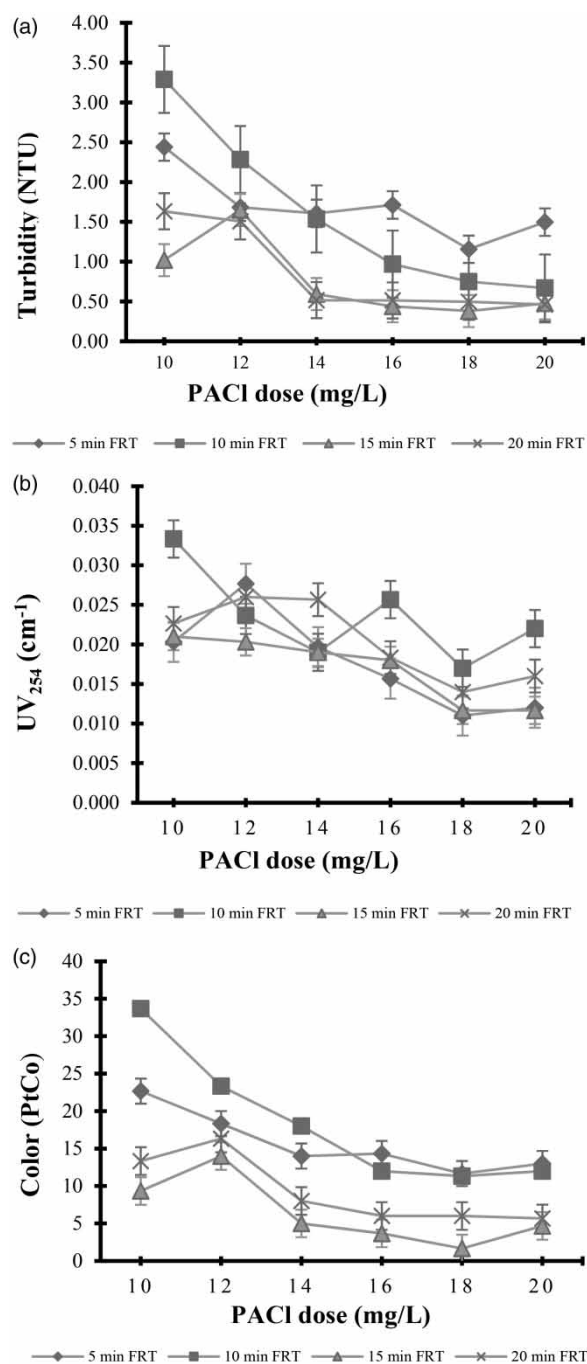

Figure 2 | Effect of varying PACl dose and FRT on Turbidity (a), UV_{254} (b) and color (c) removal.

organics could be achieved with coagulant doses ranging from 15 to 25 mg/L. It appears that the removal of organics and particulates mostly occurs at the early stages of flocculation and depending on the specific characteristics of the raw

Table 4 | Statistical results for preliminary jar test

Response	Source	Sums of squares	DF	Mean squares	F-value	p-value
Turbidity	PACl dose	18.500	5	3.7001	8.88	0.000
	FRT	13.273	3	4.4244	10.61	0.000
UV_{254}	PACl dose	0.000809	5	0.000162	2.60	0.037
	FRT	0.000712	3	0.000237	3.82	0.016
Color	PACl dose	1421.9	5	284.39	18.56	0.000
	FRT	1,832.8	3	610.93	27.87	0.000

water and the parameter being studied, there is a certain critical FRT beyond which no significant improvement in water quality can be attained. In this study, that critical FRT was observed at 15 mins. Consequently, 20 min FRT was not considered during the optimization process as a high retention time implicates higher mixing volumes as well as a higher energy consumption and yet no improvement in water quality would be attained. Therefore PACl doses ranging from 10 to 20 mg/L and FRT ranging from 5 to 15 min were used for RSM optimization.

Optimization of the hybrid coagulation-UF system

Table 5 shows the layout and results of the 2^2 CCD. Irrespective of the factor settings used in this study, the color of permeate was zero (100% removal of color forming compounds). Hence, color was deemed an inappropriate response for assessing the effect of varying PACl dose and FRT on the hybrid coagulation-UF system. Three quadratic models representing the permeate turbidity, the presence of UV_{254} absorbing organics and the permeability across the membrane were therefore obtained from the CCD and their statistical significance were examined by ANOVA. Fit summary output analysis revealed that the models were

statistically significant (*p*-value <0.05) to describe the permeate turbidity, UV_{254} and the membrane permeability.

As depicted in Table 6, the *p*-value for the mathematical model for turbidity implied that the model was highly significant. In addition to that, the multiple regression coefficient R^2 of the model was 0.9850, suggesting that 98.50% of the variability in the response could be well explained by the model. Thus, a good agreement existed between the experimental and the predicted values as only 1.50% of the variability was poorly described by the model. Moreover, the value for Lack-of-Fit was insignificant denoting that the model was reasonable fit. The normal probability and response surface plots for turbidity are displayed in Figure 3. The analysis of the CCD is based on the assumption that the observations made are independently and normally distributed. As shown by the normal probability plot, the data points were fairly close to the straight line thus depicting that the experiment came from a normally distributed population. It can also be seen from the surface plot that the permeate turbidity decreased with increasing PACl dose. The minimum turbidity (<0.15 NTU) was observed with PACl dose >20 mg/L and FRT ranging from 6–13.5 min (Figure S1, Supplement, available with the online version of this paper).

Table 5 | Two-factorial CCD layout and experimental results

			Factor variables		Response variables[c]		
Standard order[a]	Run order[b]	Blocks	X_1	X_2	Y_1 (NTU)	Y_2 (cm^{-1})	Y_3 (Lm^{-2} h^{-1}bar^{-1})
1	8	1	0.0	1.4	0.22	0.006	56.5
2	5	1	−1.4	0.0	0.25	0.007	64.6
3	3	1	−1.0	1.0	0.22	0.008	68.0
4	9	1	0.0	0.0	0.16	0.002	28.8
5	12	1	0.0	0.0	0.16	0.002	34.6
6	4	1	1.0	1.0	0.16	0.004	68.4
7	2	1	1.0	−1.0	0.18	0.001	56.6
8	7	1	0.0	−1.4	0.25	0.002	59.0
9	11	1	0.0	0.0	0.17	0.002	46.2
10	1	1	−1.0	−1.0	0.29	0.003	45.4
11	10	1	0.0	0.0	0.17	0.003	46.1
12	13	1	0.0	0.0	0.16	0.002	35.8
13	6	1	1.4	0.0	0.13	0.002	68.7

[a]Not randomized.
[b]Randomized.
[c]Mean of three readings.

Table 6 | Statistical analysis of the results of the two-factorial CCD

Response	Factors	SS	DF	MS	F-value	p-value
Turbidity	Model	0.026505	5	0.005301	92.10	0.000
	X_1	0.014425	1	0.014425	250.61	0.000
	X_2	0.002192	1	0.002192	38.08	0.000
	X_1*X_1	0.001176	1	0.001176	20.42	0.003
	X_2*X_2	0.008767	1	0.008767	152.31	0.000
	X_1*X_2	0.000625	1	0.000625	10.86	0.013
	Lack-of-Fit	0.000283	3	0.000094	3.14	0.149
	$R^2 = 0.9850$					
	R^2-Adj $=0.9743$					
UV$_{254}$	Model	0.000057	5	0.000011	45.74	0.000
	X_1	0.000021	1	0.000021	85.20	0.000
	X_2	0.000023	1	0.000023	93.01	0.000
	X_1*X_1	0.000008	1	0.000008	32.82	0.001
	X_2*X_2	0.000005	1	0.000005	19.47	0.003
	X_1*X_2	0.000001	1	0.000001	3.99	0.085
	Lack-of-Fit	0.000001	3	0.000000	1.59	0.330
	$R^2 = 0.9706$					
	R^2-Adj $= 0.9496$					
Permeability	Model	45881.3	5	9176.3	5.95	0.018
	X_1	949.0	1	949.0	0.61	0.030
	X_2	2992.8	1	2992.8	1.94	0.168
	X_1*X_1	31794.4	1	31794.4	20.60	0.003
	X_2*X_2	14285.2	1	14285.2	9.26	0.018
	X_1*X_2	718.1	1	718.1	0.47	0.517
	Lack-of-Fit	4954.3	3	1651.4	1.13	0.439
	$R^2 = 0.8100$					
	R^2-Adj $=0.6742$					

As shown in Table 6, the main effect of PACl dose (X_1), the main effect of FRT (X_2), the second order effect of PACl dose (X_1*X_1), the second order effect of FRT (X_2*X_2) and the interaction of PACl dose and FRT (X_1*X_2) were all found to be the significant factors affecting the permeate turbidity. The regression model for turbidity (Y_1) is given by Equation (7):

$$Y_1 = 0.6576 - 0.02435\,X_1 - 0.03924\,X_2$$
$$+\ 0.000365\,X_1^2 +\ 0.001421\,X_2^2 +\ 0.000420\,X_1X_2 \quad (7)$$

Apart from turbidity, UV$_{254}$ is another important response variable for this study as it was used to connote the efficiency of

pre-coagulation in removing organics from the feed water. As depicted in Table 6, the model for UV$_{254}$ was found to be very significant. Coupled with that, the R^2 showed that 97.06% of the variability in the response could be well explained by the model. Furthermore, the model was found to be satisfactory as the value for Lack-of-Fit was statistically insignificant. The normal probability and surface plot for UV$_{254}$ are shown in Figure 4. As shown in Figure 4, UV$_{254}$ removal increased with increasing PACl dose and decreasing FRT. The lowest UV$_{254}$ ($<0.002\ \mathrm{cm}^{-1}$) could be achieved with PACl dose >16 mg/L and at a retention time <11 min (Figure S2, Supplement, available online).
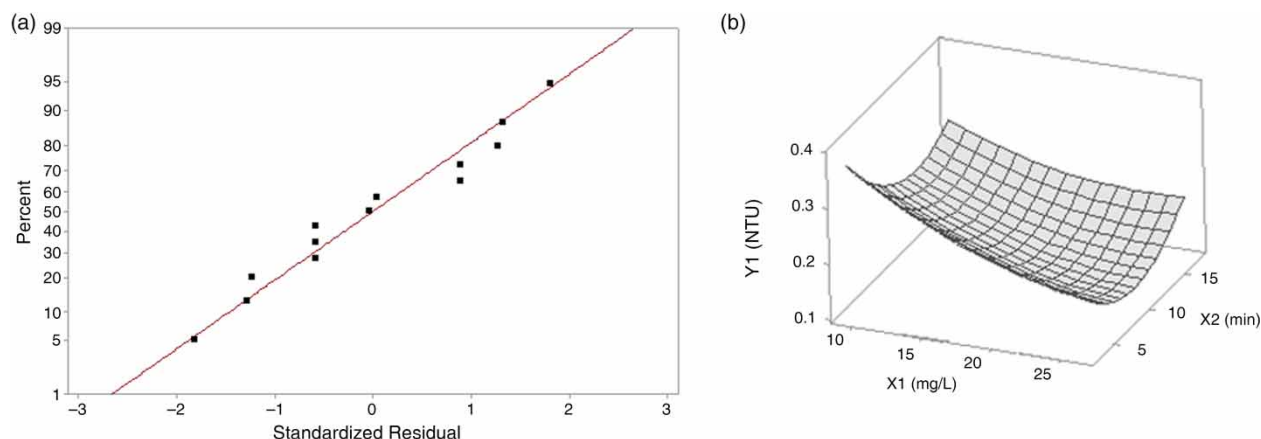
Figure 3 | Normal probability plot (a) and response surface plot (b) for turbidity.
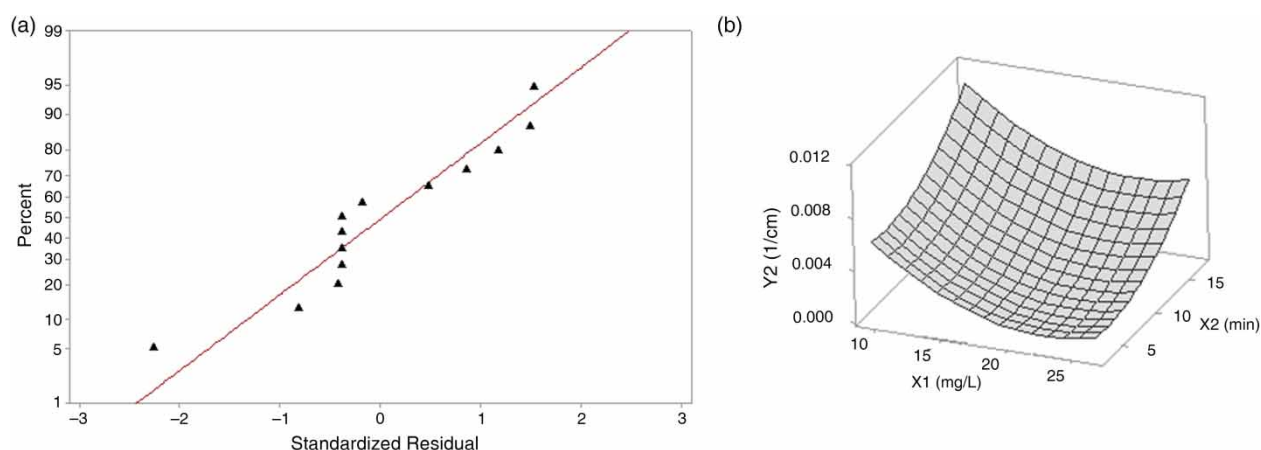

Figure 4 | Normal probability plot (a) and response surface plot (b) for UV$_{254}$ absorbance.

The significant model terms for UV$_{254}$ were the main effect of PACl dose (X_1), the second order effect of PACl dose (X_1*X_1), the main effect of FRT (X_2) and the second other effect of FRT (X_2*X_2). The two level interactions of PACl dose and FRT was statistically insignificant (*p*-value = 0.085) and was therefore eradicated using backward elimination procedures to improve the model (Table S1, Supplement, available online). Ultimately, the regression model for UV$_{254}$ absorbance (Y_2) was reduced to the form shown in Equation (8):

$$Y_2 = 0.01677 - 0.001364\,X_1 - 0.000331\,X_2 \\ + 0.000031\,X_1^2 + 0.000034\,X_2^2 \qquad (8)$$

Permeability as a third response variable was used to denote the fouling potentials of the pre-coagulated water. Less fouling is accompanied by high hydraulic permeability while the converse is true for exacerbated fouling (Bae & Tak 2005). The empirical model for permeability was also found to be statistically significant (Table 6). An R^2 of 0.8100 was computed for the regression indicating that there is a strong correlation. To cap it all, the Lack-of-Fit test did not show inadequacy of the model implying that the model could adequately fit the experimental results. The normal probability and surface plots for permeability are also shown in Figure 5. As depicted in response surface plot, permeability decreased around the center of the surface
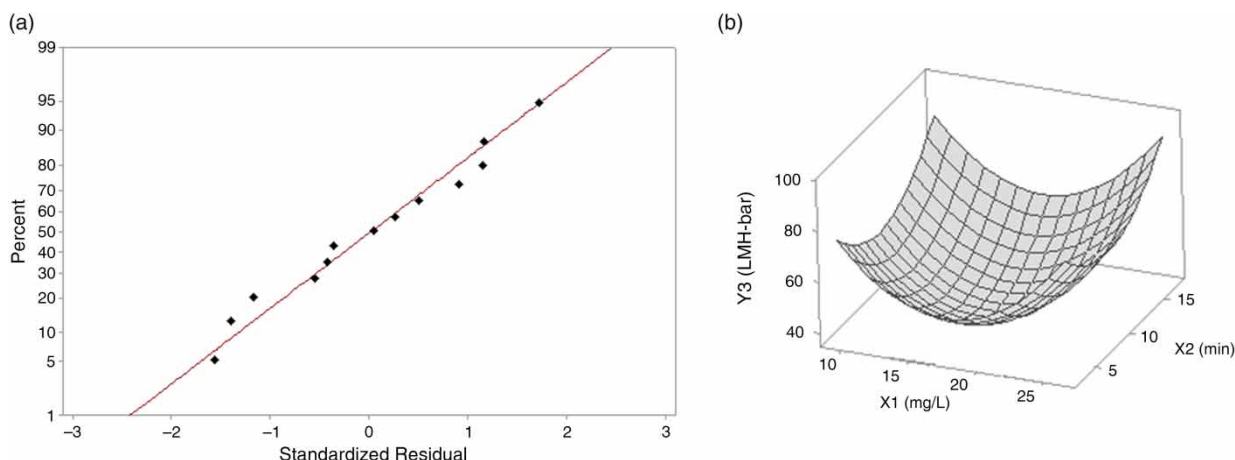
Figure 5 | Normal probability plot (a) and response surface plot (b) for permeability.

plot. The minimum permeability (28.8 $Lm^{-2} h^{-1} bar^{-1}$) was centered in the vicinity of 17 mg/L PACl and FRT of 9 min with increasing values along both sides of the point (Figure S3, Supplement, available online).

It was also revealed that within the context of this study, the main effect of PACl dose (X_1), the second order effect of PACl dose (X_1*X_1) and the second order effect of FRT (X_2*X_2) were the significant factors affecting the permeability (Table 6). Therefore to improve the model, the backwards elimination procedure was once again employed to eradicate the insignificant factors (Table S1, Supplement). The final empirical model for permeability is shown in Equation (9):

$$Y_3 = 181.4 - 13.19\,X_1 - 6.50\,X_2 + 0.3797\,X_1^2 + 0.364\,X_2^2 \quad (9)$$

The membrane permeability seemed to be dependent on a complex interaction between the coagulant dose and FRT. Coagulant doses and FRTs that formed smaller flocs had low permeability. On the other hand, coagulant doses and FRTs that formed bigger flocs contributed to high membrane permeability. This corresponds to the cake layer theory according to the Carman-Kozeny model (Equation (10)), which implies that the cake layer resistance is inversely proportional to the square of the particle diameter:

$$Kc = \frac{180 C_c^2}{d_p^2 (1 - C_c)^3} \quad (10)$$

where K_c is the specific cake resistance, C_c is solid concentration or solidosity of the cake in volume percentage and d_p is the particle diameter.

This was also observed in previous studies demonstrating that a cake layer formed by smaller particles is much compact compared to that formed by large ones, which imply that smaller particles have a higher specific cake resistance (Lin *et al.* 2011; Chomiak *et al.* 2014). In addition to that, coagulant doses and FRTs that formed bigger flocs also contributed to higher removal of UV_{254} organics. Because humic NOM has more electron rich sites (carboxylic functional groups) for bulk NOM agglomeration through charge neutralization with cationic aluminum hydrolysis, at the appropriate coagulation conditions, humic acid molecules are more readily absorbed to the surface of positively charged Al species (Choi *et al.* 2013). Better NOM agglomeration would therefore imply the formation of bigger flocs which were easily retained by the UF membrane and this explains why higher UV_{254} organics removal was observed with bigger flocs. It must also be noted that coagulant doses and FRTs that formed very tiny flocs had low permeate quality due to the permeation of smaller particles through the UF membrane.

Determination and experimental validation of the optimum results

For any given condition, a tradeoff was found between turbidity, UV_{254} and the permeate flux. High turbidity and

UV_{254} rejections were sometimes accompanied by low permeability and vice versa. This phenomenon is very evident in standard orders 4, 5 and 12 (Table 5) where turbidity of 0.16 NTU and UV_{254} absorbance of 0.002 cm^{-1} corresponded with very low permeability (28.8, 34.6 and 35.8 Lm^{-2} h^{-1} bar^{-1} for standard orders 4, 5 and 12, respectively). These results were consistent with previous studies by Zularisam *et al.* (2009) who observed a contradictory relation between the membrane permeability and NOM rejection in that an increase in NOM rejection through a single separation process sometimes led to a decrease in membrane permeability and vice versa. Hence, to simultaneously optimize the responses, a multi-criteria approach that finds the optimal compromises between turbidity, UV_{254} and membrane permeability was required to predict the optimum factor combination. Using the desirability function approach (Murphy *et al.* 2005), the composite desirability of the three responses was established (Figure S4, Supplement, available online). At this composite desirability, the predicted optimal coagulant dose and FRT were 20.07 ($\approx$20) mg/L and 13.64 ($\approx$14) min, respectively. Corresponding turbidity, UV_{254} and permeability at 95% CI were 0.15 $\pm$ 0.01 NTU, 0.0033 $\pm$ 0.0007 cm^{-1} and 62.0 $\pm$ 9.52 Lm^{-2} h^{1} bar^{-1}. In order to confirm the prediction accuracy of the empirical models, the adequacy of the models were validated through experiments. Experimental confirmation runs under the optimized conditions confirmed the validity of the models as the results of the experiment closely agreed with the models' predictions (Table 7). In addition to that there was no significant difference ($p > 0.05$) between the predicted and observed values. Thus the models can be reliably used to predict the quality and quantity of permeate from the hybrid coagulation-UF membrane process of feed water from Lake Victoria at the experimental scale.

It should be kept in mind that the present model is focused on permeability, turbidity and UV_{254} removal only. For practical implementation of the coagulation-UF process, the end points which need to be optimized actually are water quality (turbidity, organics, pathogen count) and total annual costs. Membrane flux influences investment costs and capital costs (depreciation). However, total costs are furthermore related to the consumption of chemicals, including coagulant and cleaning chemicals, and other factors such as labor and maintenance. These factors depend highly on locally and dependent variables such as interest rate and wages. Thus, optimizing operation costs is far more complex and exceeds the framework of this study. However, in principle a similar approach can be used whereby the desirability is extended with functions describing capital costs and the costs for chemical usage and labor (cleaning operations) in order to optimize the overall feasibility of the coagulation-UF process.

Table 7 | Comparison between predicted and observed values for turbidity, UV_{254} absorbance and membrane permeability

Optimized condition[a]	
Dose (mg/L)	20.07 ($\approx$20)
FRT (min)	13.643 ($\approx$14)
Predicted values[b]	
Turbidity (NTU)	0.15 $\pm$ 0.01
UV_{254} absorbance (cm^{-1})	0.0033 $\pm$ 0.0007
Permeability (Lm^{-2} h^{-1} bar^{-1})	62.0 $\pm$ 9.52
Observed values[c]	
Turbidity (NTU)	0.15 $\pm$ 0.01
UV_{254} absorbance (cm^{-1})	0.0030 $\pm$ 0.0010
Permeability (Lm^{-2} h^{-1} bar^{-1})	59.0 $\pm$ 2.1

[a]Obtained from desirability function.
[b]Mean $\pm$ CI.
[c]Mean $\pm$ CI ($n = 4$).

CONCLUSIONS

The optimum operating conditions for a hybrid PACl coagulation-UF system for treating potable water from Lake Victoria were obtained using RSM. The focus of the study was to establish the optimum PACl dose and FRT for enhancing both organic and inorganic matter removal while simultaneously optimizing membrane permeability. Using RSM models, the optimum PACl dose and FRT for the feed water were 20.07 ($\approx$20) mg/L and 13.64 ($\approx$14) min, respectively. At this factor combination, turbidity, UV_{254} and permeability of 0.15 $\pm$ 0.01 NTU, 0.0030 $\pm$ 0.0010 cm^{-1} and 62.0 $\pm$ 9.52 Lm^{-2} h^{-1} bar^{-1} were respectively predicted. Experimental validations confirmed the reliability of these predicted optimum settings, indicating that RSM models can be used to predict optimum operating conditions for hybrid coagulation-UF process of the feed water at the bench scale.

The effectiveness of the hybrid system appears to be influenced by a complex interaction between the coagulant dose and FRT. Coagulant doses and FRTs that formed smaller flocs offered high hydraulic resistance which led to low membrane permeability whereas agglomeration of particles into bigger flocs contributed to high membrane permeability. Also, smaller flocs led to low turbidity and UV_{254} rejection while the converse was true for bigger flocs. However, a trade-off was found between the permeate turbidity, UV_{254} and the permeability in that increase in one sometimes led to a decrease in the other. Consequently, a multi-criteria approach that finds the optimal compromises between turbidity, UV_{254} and membrane permeability was used to simultaneously optimize the responses. This demonstrates that to maximize production, coagulation conditions should be set in order to achieve the optimum compromise between floc size, solute rejection and membrane permeability. The results presented here provide insights into simultaneous optimization of relevant operating factors in pilot or full scale coagulation-UF plants for drinking water treatment.

ACKNOWLEDGEMENTS

REFERENCES

Amy, G. 2008 Fundamental understanding of organic matter fouling of membranes. *Desalination* **231** (1–3), 44–51.

Arhin, S. G., Banadda, N., Komakech, A. J., Kabenge, I. & Wanyama, J. 2016 Membrane fouling control in low pressure membranes : a review on pretreatment techniques for fouling abatement. *Environmental Engineering Research* **21** (2), 109–120.

ASTM International D2035 2013 *Standard Practice for Coagulation-Flocculation Jar Test of Water*, ASTM International, West Conshohocken, PA, USA.

Bae, T. H. & Tak, T. M. 2005 Interpretation of fouling characteristics of ultrafiltration membranes during the filtration of membrane bioreactor mixed liquor. *Journal of Membrane Science* **264** (1), 151–160.

Bas, D. & Boyaci, I. H. 2007 Modeling and optimization I : usability of response surface methodology. *Journal of Food Engineering* **78** (3), 836–845.

Bergamasco, R., Konradt-Moraes, L. C., Vieira, M. F., Fagundes-Klen, M. R. & Vieira, A. M. S. 2011 Performance of a coagulation-ultrafiltration hybrid process for water supply treatment. *Chemical Engineering Journal* **166** (2), 483–489.

Bezerra, M. A., Santelli, R. E., Oliveira, E. P., Villar, L. S. & Escaleira, L. A. 2008 Response surface methodology (RSM) as a tool for optimization in analytical chemistry. *Talanta* **76** (5), 965–977.

Cho, M. H., Lee, C. H. & Lee, S. 2006 Effect of flocculation conditions on membrane permeability in coagulation-microfiltration. *Desalination* **191** (1–3), 386–396.

Choi, K. Y. & Dempsey, B. A. 2004 In-line coagulation with low-pressure membrane filtration. *Water Research* **38** (19), 4271–4281.

Choi, Y. H., Nason, J. A. & Kweon, J. H. 2013 Effects of aluminum hydrolysis products and natural organic matter on nanofiltration fouling with PACl coagulation pretreatment. *Separation & Purification Technology* **120**, 78–85.

Chomiak, A., Mimoso, J., Koetzsch, S., Sinnet, B., Pronk, W., Derlon, N. & Morgenroth, E. 2014 Biofilm formation and permeate quality improvement in gravity driven membrane ultrafiltration. *Water Science & Technology: Water Supply* **14** (2), 274–282.

Chon, K., Kim, S. J., Moon, J. & Cho, J. 2012 Combined coagulation-disk filtration process as a pretreatment of ultrafiltration and reverse osmosis membrane for wastewater reclamation: an autopsy study of a pilot plant. *Water Research* **46** (6), 1803–1816.

Dong, B. Z., Chen, Y., Gao, N. Y. & Fan, J. C. 2007 Effect of coagulation pretreatment on the fouling of ultrafiltration membrane. *Journal of Environmental Science* **19** (3), 278–283.

Duan, J. & Gregory, J. 2003 Coagulation by hydrolysing metal salts. *Advances in Colloids & Interface Science* **100**, 475–502.

Fiksdal, L. & Leiknes, T. 2006 The effect of coagulation with MF/UF membrane filtration for the removal of virus in drinking water. *Journal of Membrane Science* **279** (1), 364–371.

Gamage, N. P. & Chellam, S. 2011 Aluminum electrocoagulation pretreatment reduces fouling during surface water microfiltration. *Journal of Membrane Science* **379** (1), 97–105.

Gao, W., Liang, H., Ma, J., Han, M., Chen, Z., Han, Z. & Li, G. 2011 Membrane fouling control in ultrafiltration technology for drinking water production: a review. *Desalination* **272** (1), 1–8.

Guo, X., Zhang, Z., Fang, L. & Su, L. 2009 Study on ultrafiltration for surface water by a polyvinylchloride hollow fiber membrane. *Desalination* **238** (1–3), 183–191.

Hatt, J. W., Germain, E. & Judd, S. J. 2011 Water treatment using hybrid method of coagulation and low-pressure membrane filtratio. *Water Research* **45** (1), 6471–6478.

Hill, V. R., Kahler, A. M., Jothikumar, N., Johnson, T. B., Hahn, D. & Cromeans, T. L. 2007 Multistate evaluation of an ultrafiltration-based procedure for simultaneous recovery of enteric microbes in 100-liter tap water samples. *Applied & Environmental Microbiology* **73** (13), 4218–4225.

Howe, K. J. & Clark, M. M. 2006 Effect of coagulation pretreatment on membrane filtration performance. *Journal of American Water Works Association* **98** (4), 133–146.

Jeong, S., Choi, Y. J., Nguyen, T. V., Vigneswaran, S. & Hwang, T. M. 2012 Submerged membrane hybrid systems as pretreatment in seawater reverse osmosis (SWRO): optimisation and fouling mechanism determination. *Journal of Membrane Science* **411**, 173–181.

Kim, H.-S., Takizawa, S. & Ohgaki, S. 2007 Application of microfiltration systems coupled with powdered activated carbon to river water treatment. *Desalination* **202** (1–3), 271–277.

Kimura, K., Tanaka, K. & Watanabe, Y. 2014 Microfiltration of different surface waters with/without coagulation: clear correlations between membrane fouling and hydrophilic biopolymers. *Water Research* **49**, 434–443.

Konieczny, K., Bodzek, M. & Rajca, M. 2006 A coagulation-MF system for water treatment using ceramic membranes. *Desalination* **198** (1–3), 92–101.

Konieczny, K., Rajca, M., Bodzek, M. & Kwiecinska, A. 2009 Water treatment using hybrid method of coagulation and low-pressure membrane filtration. *Environmental Protection Engineering* **35** (1), 5–22.

Lai, C., Chou, Y. & Yeh, H. 2015 Assessing the interaction effects of coagulation pretreatment and membrane material on UF fouling control using HPSEC combined with peak-fitting. *Journal of Membrane Science* **474**, 207–214.

Li, M., Wu, G., Guan, Y. & Zhang, X. 2011 Treatment of river water by a hybrid coagulation and ceramic membrane process. *Desalination* **280** (1–3), 114–119.

Liang, H., Gong, W., Chen, J. & Li, G. 2008 Cleaning of fouled ultrafiltration (UF) membrane by algae during reservoir water treatment. *Desalination* **220** (1–3), 267–272.

Lin, H. J., Gao, W. J., Leung, K. T., Liao, B. Q. & Lin, H. J. 2011 Characteristics of different fractions of microbial flocs and their role in membrane fouling. *Water Science & Technology* **63** (2), 262–269.

Maartens, A., Swart, P. & Jacobs, E. P. 1999 Feed-water pretreatment: methods to reduce membrane fouling by natural organic matter. *Journal of Membrane Science* **163** (1), 51–62.

Meng, F., Zhang, H., Yang, F., Li, Y., Xiao, J. & Zhang, X. 2006 Effect of filamentous bacteria on membrane fouling in submerged membrane bioreactor. *Journal of Membrane Science* **272** (1), 161–168.

Mimoso, J., Pronk, W., Morgenroth, E. & Hammes, F. 2015 Bacterial growth in batch-operated membrane filtration systems for drinking water treatment. *Separation & Purification Technology* **156**, 165–174.

Mull, B. & Hill, V. R. 2012 Recovery of diverse microbes in high turbidity surface water samples using dead-end ultrafiltration. *Journal of Microbiological Methods* **91** (3), 429–433.

Munla, L., Peldszus, S. & Huck, P. M. 2012 Reversible and irreversible fouling of ultrafiltration ceramic membranes by model solutions. *Journal of American Water Works Association* **104** (10), 540–554.

Murphy, T. E., Tsui, K. & Allen, J. K. 2005 A review of robust design methods for multiple responses. *Research in Engineering Design* **16** (4), 118–132.

Prasad, K. N., Abdulrahman, F., Yang, B., Weng, K., Nagasundara, R., Azlan, A. & Ismail, A. 2011 Response surface optimisation for the extraction of phenolic compounds and antioxidant capacities of underutilised *Mangifera pajang* Kosterm peels. *Food Chemistry* **128** (4), 1121–1127.

Sharma, S., Malik, A. & Satya, S. 2009 Application of response surface methodology (RSM) for optimization of nutrient supplementation for Cr (VI) removal by Aspergillus lentulus AML05. *Journal of Hazardous Materials* **164** (2), 1198–1204.

Silva, E. M., Rogez, H. & Larondelle, Y. 2007 Optimization of extraction of phenolics from Inga edulis leaves using response surface methodology. *Separation & Purification Technology* **55** (3), 381–387.

USEPA Method 415.3 2003 *Determination of Total Organic Carbon and Specific UV Absorbance at 254 nm in Source Water and Drinking Water*, US Environmental Protection Agency, Cincinnati, OH, USA.

Xiangli, Q., Zhenjia, Z., Nongcun, W., Wee, V., Low, M., Loh, C. S. & Teck Hing, N. 2008 Coagulation pretreatment for a large-scale ultrafiltration process treating water from the Taihu River. *Desalination* **230** (1–3), 305–313.

Xu, H., Chen, W., Xiao, H. & Hu, X. 2014 Stability of an ultrafiltration system for drinking water treatment, using chlorine for fouling control. *Desalination* **336**, 187–195.

Zularisam, A. W., Ismail, A. F., Salim, M. R., Sakinah, M. & Matsuura, T. 2009 Application of coagulation – ultrafiltration hybrid process for drinking water treatment : optimization of operating conditions using experimental design. *Separation & Purification Technology* **65** (2), 193–210.